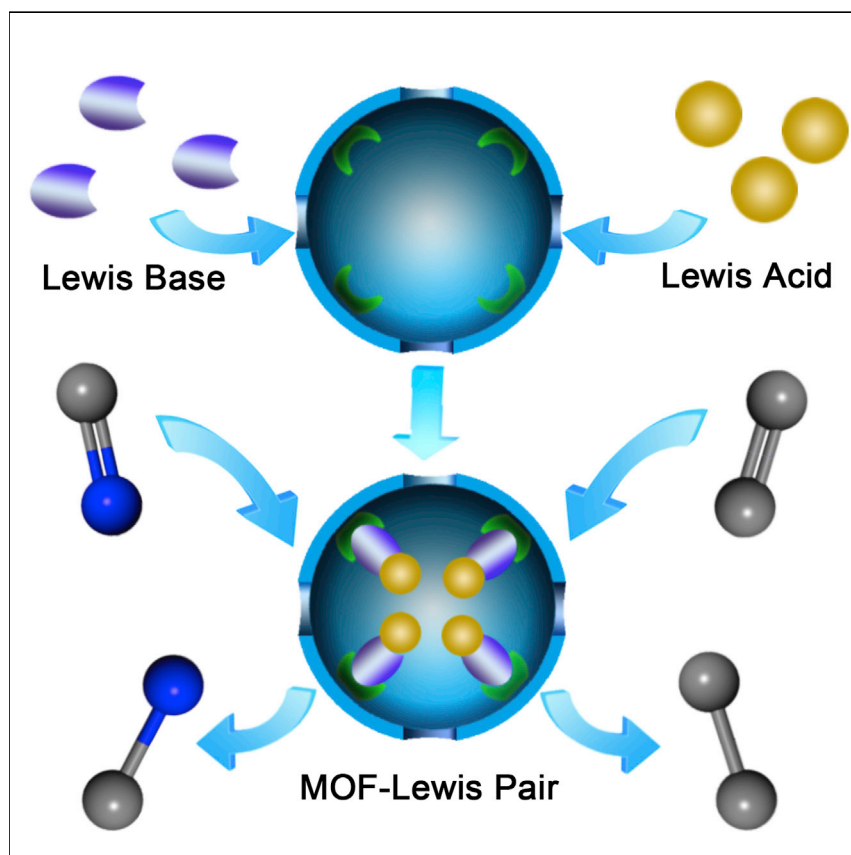


Article

Metal-Organic Framework Anchored with a Lewis Pair as a New Paradigm for Catalysis



Lewis pairs (LPs), classical and frustrated, have been successfully introduced into and stabilized in a metal-organic framework (MOF). Benefiting from the robust framework and tunable porous structure of MOFs, the resultant MOF-LP demonstrates not only great recyclability but also excellent performance in the catalytic reduction of imines and hydrogenation of alkenes. The combination of LP and MOF therefore lays a foundation for developing a MOF-LP as a new paradigm for catalysis, particularly heterogeneous catalysis.

Zheng Niu, Wilarachchige D.C. Bhagya Gunatilleke, Qi Sun, ..., Yuchuan Cheng, Briana Aguila, Shengqian Ma

sqma@usf.edu

HIGHLIGHTS

A stepwise strategy was developed to anchor the Lewis pair (LP) in a MOF

MOF-LP shows excellent catalytic performance for reduction of imines and alkenes

MOF-LP-catalyzed reduction reactions show unique size and steric selectivity

MOF-LP demonstrates excellent recycling performance



Niu et al., Chem 4, 2587–2599
November 8, 2018 © 2018 Elsevier Inc.
<https://doi.org/10.1016/j.chempr.2018.08.018>



Article

Metal-Organic Framework Anchored with a Lewis Pair as a New Paradigm for Catalysis

Zheng Niu,¹ Wilarachchige D.C. Bhagya Gunatilleke,¹ Qi Sun,¹ Pui Ching Lan,¹ Jason Perman,¹ Jian-Gong Ma,² Yuchuan Cheng,³ Briana Aguila,¹ and Shengqian Ma^{1,4,*}

SUMMARY

Lewis pair (LP) chemistry has shown broad applications in the catalysis field. However, one significant challenge has been recognized as the instability for most homogeneous LP catalysts upon recycling, thus inevitably leading to dramatic loss in catalytic activity. Additionally, current heterogeneous LP catalysts suffer from low surface area, which largely limits their catalytic efficiency, thereby restricting their potential applications. In this work, we report the successful introduction of LPs, classical and frustrated, into a metal-organic framework (MOF) that features high surface and ordered pore structure via a stepwise anchoring strategy. Not only can the LP be stabilized by the strong coordination interaction between the LP and MOF, but the resultant MOF-LP also demonstrates excellent catalysis performance with interesting size and steric selectivity. Given the broad applicability of LPs, our work therefore paves a way for advancing MOF-LP as a new paradigm for catalysis.

INTRODUCTION

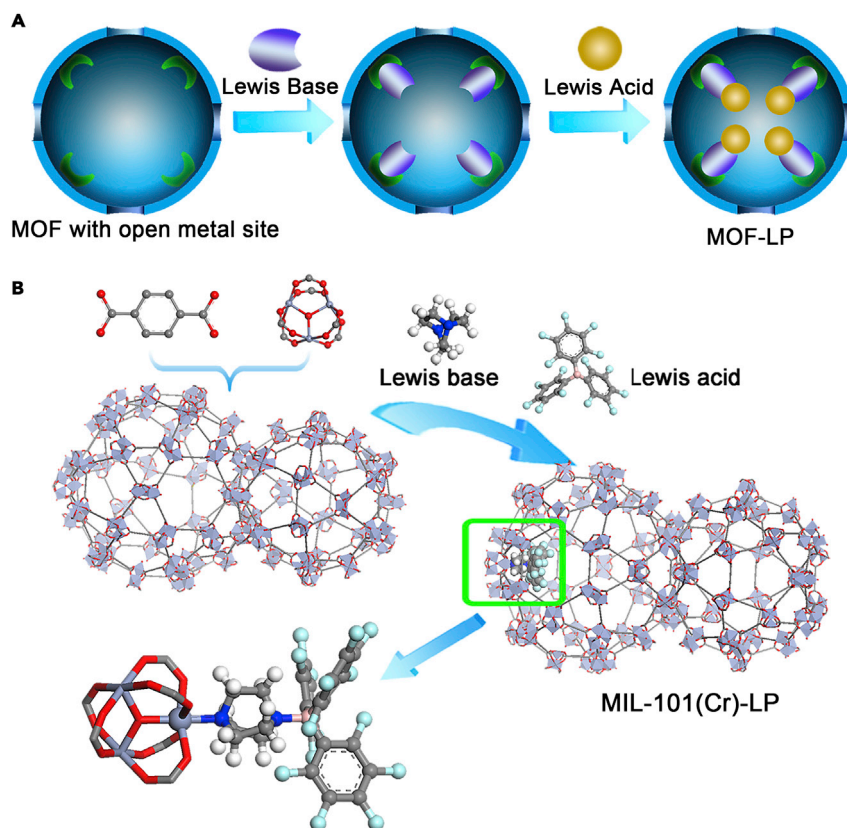
Increasing attention has recently been drawn to Lewis pair (LP) chemistry because of its broad applicability, from theoretical chemistry to catalysis and synthetic chemistry.^{1–6} One important part of LPs is that they exhibit wide applications in catalytic polymerization,^{7,8} C–H bond activation,⁹ and catalytic reduction fields.^{10,11} However, the instability of most LP catalysts upon recycling inevitably leads to the dramatic loss in catalytic activity. Meanwhile, the low surface area of current heterogeneous LP catalysts limits their catalytic efficiency, thereby restricting their industrial applications. Loading the catalysts into porous materials^{12,13} would be a short-cut method to obtain better recycling performance and catalytic efficiency than current catalysts but has not yet been achieved, presumably because of the lack of anchoring sites to hold and stabilize the LPs in most porous material supports.

As one attractive type of porous crystalline material, metal-organic frameworks (MOFs) have shown enormous potential in catalysis areas due to their well-defined yet tunable pores and functionalized walls.^{14–18} The suitable pore size, high surface area, and spacious pore space of MOFs can provide the substrate molecules enough accessibility with the catalytic centers inside MOFs.¹⁹ Via directly utilizing^{20–23} or post-synthetically functionalizing^{24–26} the linkers or secondary building units (SBUs), MOFs have been extensively investigated as single-site heterogeneous catalysts.^{27–30} Meanwhile, taking advantage of their spacious pore space and tunable pore sizes, MOFs have also been widely used to support various catalytic species, such as organometallic complexes,^{31–33} nanoparticles,^{34–39} and enzymes,^{40–42} for

The Bigger Picture

Lewis pairs (LPs), classical and frustrated, are excellent prospects in catalysis, organic syntheses, biology, and material sciences. However, the instability of most LP catalysts leads to a dramatic loss in activities, thereby largely restricting their industrial applications. As robust porous materials, metal-organic frameworks (MOFs) offer a platform to stabilize homogeneous catalysts. Here, we show a strategy that grafts the LP catalyst on the MOF to minimize loss of LPs during catalysis and recycling. Our work reveals the enormous potential of MOFs as an appealing paradigm for the construction of efficient heterogeneous catalysts with interesting steric and size selectivity worthy of exploration. In addition, the strategies for anchoring a LP into a MOF as contributed herein can be readily applied for the task-specific design of functional catalysis materials for various applications.





Scheme 1. Introduction of the LP into the MOF

(A) Illustration of the stepwise anchoring strategy for grafting the LP on the open metal site of the MOF.

(B) Construction pathway of MIL-101(Cr)-LP.

heterogeneous catalysis. The merits of MOFs would make them a promising type of scaffold to stabilize LPs, which has recently been suggested by computational studies⁴³ but has not yet been realized experimentally. This could be likely due to the fact that most LP catalysts are very water sensitive,^{44–46} and thereby the active species would decompose during the MOF synthesis process when a ligand functionalized with LP moieties is used.

RESULTS

Introduction of the LP into the MOF

To tackle the above issues, we contribute a strategy that allows the successful grafting of the LP into the MOF. As illustrated in Scheme 1A, the custom-designed base moiety of the LP is first anchored to the open metal sites within the MOF through coordination interaction, which is followed by the introduction of the corresponding acid moiety of the LP. Given the strong coordination interaction, it is anticipated that the LP would be stabilized within the MOF yet accessible to substrates.

As a proof of concept, we selected dehydrated MIL-101(Cr), $\text{Cr}_3(\text{OH})\text{O}(\text{BDC})_3$ (BDC = 1,4-benzenedicarboxylate), to anchor LP considering its large pores or cages, abundant open metal sites upon activation, and high stability^{47–50}; the LP, composed of $\text{B}(\text{C}_6\text{F}_5)_3$ and 1,4-diazabicyclo[2.2.2]octane (DABCO) that features one potential coordination site, is used as a model for grafting into the MOF. This

¹Department of Chemistry, Institution University of South Florida, 4202 E. Fowler Avenue, Tampa, FL 33620, USA

²Department of Chemistry, Institution Key Laboratory of Advanced Energy Materials Chemistry and Collaborative Innovation Center of Chemical Science and Engineering, Nankai University, Tianjin 300071, P.R. China

³Ningbo Institute of Materials Technology and Engineering, Chinese Academy of Sciences, Ningbo, Zhejiang 315201, P.R. China

⁴Lead Contact

*Correspondence: sqma@usf.edu

<https://doi.org/10.1016/j.chempr.2018.08.018>

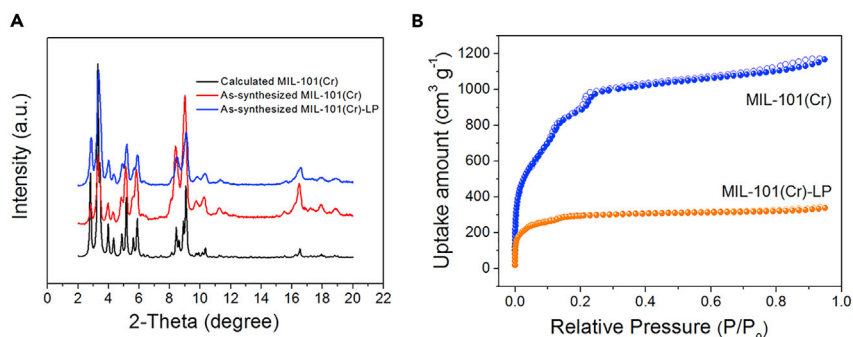


Figure 1. Structure Characterization of MIL-101(Cr)-LP

(A) PXRD of MIL-101(Cr) and MIL-101(Cr)-LP.

(B) N₂ sorption isotherms of MIL-101 and MIL-101(Cr)-LP at 77 K.

LP reacts not only with neutral borane pinacolborane (HBPin) to afford a borenium salt capable of reducing imine compounds¹⁰ but also with H₂ gas to catalyze the hydrogenation of alkylidene malonates as a frustrated LP (FLP).⁵¹ Scheme 1B shows the stepwise grafting of DABCO and B(C₆F₅)₃ into MIL-101 (Cr) and the resultant MIL-101 (Cr) anchored with B(C₆F₅)₃/DABCO pair is named MIL-101(Cr)-LP. With the LP anchored and stabilized within the nanospace of the MOF, MIL-101(Cr)-LP can efficiently catalyze both the imine reduction with interesting size and steric selectivity and the hydrogenation of alkylidene malonates directly by using H₂. Our work represents a unique example of an active and reusable LP-based heterogeneous catalyst with both size and steric selectivity, thereby opening a paradigm for catalysis.

MIL-101(Cr) was synthesized and activated according to the literature.⁵² MIL-101(Cr)-LP was prepared through a stepwise method: the activated MIL-101(Cr) was soaked into a Lewis base toluene solution, then washed, filtered, and dried under vacuum; subsequently, the solution of B(C₆F₅)₃ (Lewis acid) was added to the sample, stirred for several hours, and then washed with fresh toluene several times until no LP traces could be detected in the filtrate by liquid nuclear magnetic resonance (NMR) measurement. This process excludes the influence of the adsorbed free LP molecules in the pores of the framework. Since the theoretical maximum loading amount of anchored LP on MIL-101(Cr) is 1.47 mmol LP per 1 g MIL-101(Cr) (Figure S1), MIL-101(Cr)-LP (1 mmol LP per 1 g MIL-101(Cr) or 0.34 LP per unsaturated Cr site) was used in the following characterization.

Structure Characterization of MIL-101(Cr)-LP

The phase purity of MIL-101(Cr)-LP was verified through powder X-ray diffraction (PXRD) measurements, and the porosity of the materials was studied by N₂ gas sorption at 77 K. As shown in Figure 1A, the PXRD patterns of MIL-101(Cr)-LP are consistent with the calculated ones and those of the pristine MIL-101(Cr), indicating the preservation of the framework structure during the loading process. The N₂ sorption studies (Figure 1B) reveal that, in comparison with MIL-101, there is an obvious decrease in the Brunauer-Emmett-Teller surface area (from 2,724 to 1,013 m²/g) and reduction in pore sizes (Figures S6 and S7) for MIL-101(Cr)-LP because the LP molecules are grafted onto the pores of MIL-101(Cr) (Figure 1B).

Characterization of Anchored LP in MIL-101(Cr)-LP

The combination of LP and MIL-101 was confirmed by Fourier transform infrared spectroscopy (FTIR) analysis. The spectrum of MIL-101(Cr)-LP exhibits characteristic

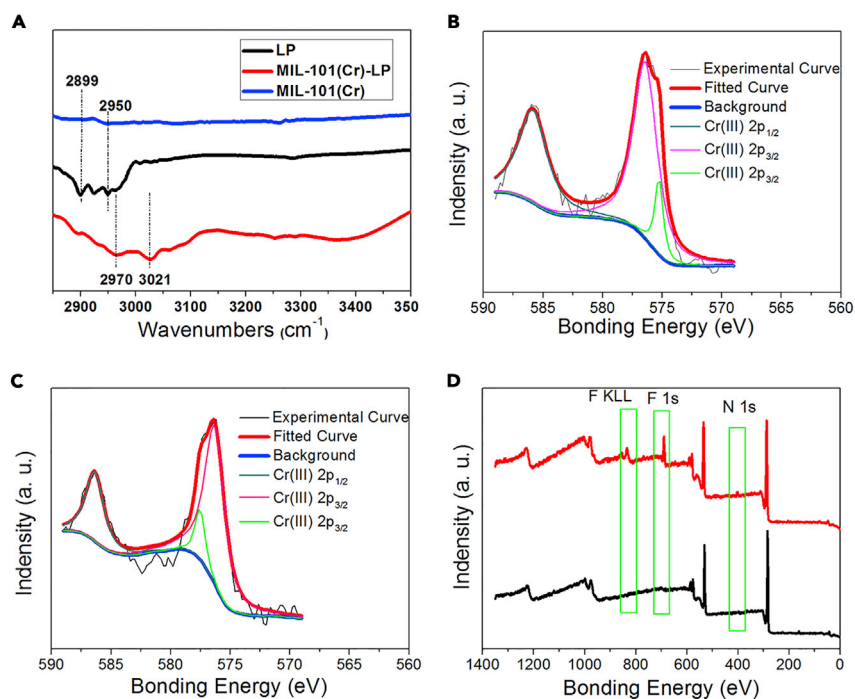


Figure 2. Characterization of Anchored LP in MIL-101(Cr)-LP

- (A) Infrared spectra of MIL-101(Cr), LP, and MIL-101(Cr)-LP.
(B) Cr(III)2p XPS spectra of MIL-101.
(C) Cr(III)2p XPS spectra of MIL-101(Cr)-LP.
(D) Survey XPS spectra of MIL-101 and MIL-101(Cr)-LP.

peaks from the LP. As shown in Figure 2A, the presence of new bands at high wavenumbers ($2,800\text{--}3,200\text{ cm}^{-1}$) is due to the aliphatic C–H stretching vibrations of the LP. Some obvious shifts are observed between MIL-101(Cr)-LP and the original LP complex (from 2,899 and 2,950 to 2,970 and 3,021 cm^{-1}), indicating a coordination interaction between the N atom of the LP and the metal site of MIL-101(Cr).^{53,54} The characteristic LP band at 1,455 cm^{-1} is slightly shifted to 1,463 cm^{-1} after the LP is loaded within the MOF (Figures S10 and S11), further suggesting possible coordination interaction between the LP and the MIL-101 framework.

X-ray photoelectron spectroscopy (XPS) spectra of MIL-101(Cr) and MIL-101(Cr)-LP were used to further verify the coordination interaction between the LP and the Cr open metal sites in MIL-101(Cr). As shown in Figures 2B and 2C, the Cr(2p) spectra of MIL-101(Cr)-LP are obviously different from the Cr(2p) spectra of MIL-101(Cr). The Cr ($2p_{1/2}$) and Cr ($2p_{3/2}$) peaks of MIL-101(Cr)-LP are shifted by about 0.58–2 eV toward higher binding energies, compared with those of MIL-101(Cr). Such shifts indicate an increase in the electron density of Cr(III), which can be attributed to the interaction between Cr and DABCO. The survey spectra of MIL-101(Cr)-LP indicate the existence of the F and N elements of the LP molecule within the MOF (Figure 2D).

Scanning electron microscopy (SEM) and transmission electron microscopy (TEM) were used to investigate the morphology of MIL-101(Cr)-LP. As shown in Figures 3A and 3B, the SEM and TEM images exhibited regular octahedral crystals of MIL-101(Cr)-LP with an average diameter of $\sim 100\text{ nm}$. For investigating the distribution of LP in MIL-101(Cr)-LP, high-angle annular dark-field scanning TEM (HAADF-STEM), and energy dispersive X-ray spectroscopy (EDS) elemental mapping analyses were

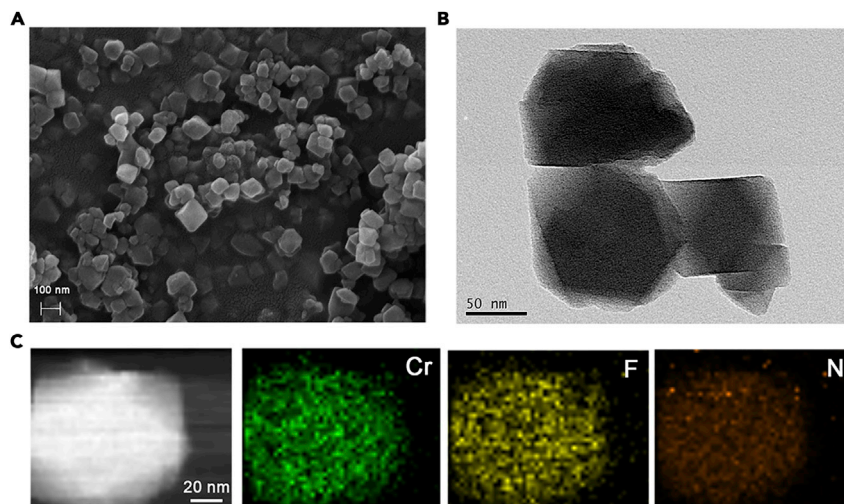


Figure 3. Morphology Characterization and Element Distribution of MIL-101(Cr)-LP

SEM image (A), TEM image (B), and HAADF-STEM image of MIL-101(Cr)-LP with the corresponding elemental mapping images (C).

used. As presented in Figure 3D, the Cr, F, and N elements are evenly distributed inside the octahedral crystal of MIL-101(Cr)-LP, suggesting the integration of LP inside the pores of the MOF. Furthermore, SEM and EDS elemental mapping analyses (Figure S12) also revealed an even distribution of B, F, and N in large scale. These results indicated that the LP was homogeneously distributed in the MIL-101(Cr) pores without the presence of accumulation in the particular regions.

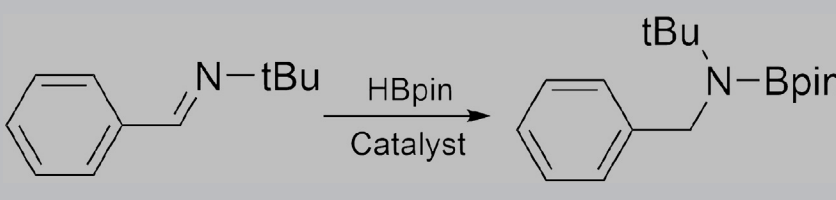
Affection of LP Loading Amount to Catalysis Performance

Compared with the expensive and potentially toxic metal-based catalyst, the metal-free LPs are shown to have enhanced catalytic performance in the synthesis of B-containing organic compounds.^{55,56} To examine the catalytic performances of LP loaded MIL-101(Cr), we prepared MIL-101(Cr)-LP-1 (0.5 mmol LP per 1 g MIL-101(Cr) or 0.17 LP per unsaturated Cr site) and MIL-101(Cr)-LP-2 (0.75 mmol LP per 1 g MIL-101(Cr) or 0.26 LP per unsaturated Cr site) to investigate the optimal uptake amount for catalyzing the imine reduction reactions. The loading amount of LP in MIL-101(Cr)-LP was quantified with ¹H NMR by decomposing MIL-101(Cr)-LP in 5 wt % NaOH D₂O solution (Figures S2–S4) and later confirmed by elemental analysis (Table S1). The pore size of these catalysts was studied through N₂ isotherms at 77 K (Figures S5, S8, and S9). The catalytic performances of the MIL-101(Cr)-LP catalysts were evaluated by exposing *N*-tert-butyl-1-phenylmethanimine (**1a**) to 1.2 equiv of HBPIn and 20 mg catalyst in toluene to result in the reduction to the corresponding pinacolboramide after 2 hr. As shown in Table 1, the lowest LP uptake amount sample, MIL-101(Cr)-LP-1, gave 83% yield, whereas MIL-101(Cr)-LP exhibited full conversion. Therefore, MIL-101(Cr)-LP was chosen for subsequent studies. The control experiment using pristine MIL-101(Cr) was conducted, but no reduction product was detected in the reaction solvent even after 48 hr, meaning that MIL-101 is inactive for the imine reduction reaction.

Catalysis Studies for Reduction of Different Imine Compounds

Imine compounds with different substituting groups were used to investigate the difference in catalysis property between the heterogeneous MIL-101(Cr)-LP and homogeneous LP counterpart. As shown in Table 2, the reaction yields catalyzed by

Table 1. Investigation of MIL-101(Cr) and MIL-101(Cr)-LP in the Catalytic Reduction of Imine 1a



Entry	Catalyst	Yield ^a
1	MIL-101(Cr)	0% ^b
2	MIL-101(Cr)-LP-1	83%
3	MIL-101(Cr)-LP-2	91%
4	MIL-101(Cr)-LP	100%

Reaction conditions: 20 mg catalyst, 55 mg (0.43 mmol) HBPIn, 56 mg (0.35 mmol) **1a**, 3 mL toluene, room temperature, 2 hr.

^aYields were determined by liquid NMR.

^bReaction time: 48 hr.

MIL-101(Cr)-LP from related imine compounds are 38% for *N*-benzylideneaniline (**2a**), 100% for *N*-benzylidene-1-phenylmethanimine (**3a**), and 22% for acridine (**4a**). For comparison, the yields are 87%, 85%, and 91% catalyzed by 3.5 mol % homogeneous LP catalyst, respectively. The comparison of the yields of these products reveals a very interesting phenomenon: the reduction product yields of **1a** and **3a** are similar or even higher than the homogeneous LP catalyst, which clearly indicates that MIL-101(Cr)-LP has comparable performance with the homogeneous LP for catalytic imine reduction with HBPIn at the same conditions; however, the reduction product yields of **2a** and **4a** are much less than the homogeneous LP catalyst. The catalysis results reveal that the steric effect close to the N atoms shows more obvious selectivity in MIL-101(Cr)-LP than LP homogeneous catalyst. This kind of steric selectivity could presumably be due to the confinement effect imparted by the porous MOF structure, which restricts the accessibility of buried C=N double bonds to the LP active centers that are anchored on the pore walls of MOF.

With the increase in the size of the imine substrate, the reduction reaction yield decreased. The reaction yield catalyzed by homogeneous LP for *N*-benzhydryl-1-phenylmethanimine (**5a**) and *N*-(diphenylmethylene)-1,1-diphenylmethanimine (**6a**) are 60% and 29%, respectively. However, the reaction yield for **5a** is 42% and none of the product could be observed in the heterogeneous MIL-101(Cr)-LP-catalyzed reaction for **6a** even after 24 hr. The high size selectivity performance can be attributed to the window structure in MIL-101(Cr)-LP. Considering the existence of the coordinated LP on the window, the size of the window (with diameter of ~1.0 nm) could be smaller than the diameter of the **6a** molecule (with diameter of 1.3 nm), thus the large imine molecule could not enter into the pore of MIL-101(Cr)-LP.

Catalysis Studies for Hydrogenation of Alkylidene Malonate Compounds

FLPs show remarkable reactivity toward the activation of the H₂ molecule.⁵⁷ However, the FLP-promoted catalytic hydrogenation of electron-poor unsaturated compounds still faces a significant challenge.⁵⁸ In view of the interesting catalytic performance of MIL-101(Cr)-LP in the above imine reduction reactions, MIL-101(Cr)-LP was used to achieve the catalytic hydrogenation of alkylidene malonates, which is one important kind of electron-poor unsaturated compound,

Table 2. Catalysis Studies for Reduction of C=N Double Bonds

Reaction scheme: $R_1R_2C=N-R_3 \xrightarrow[20 \text{ mg MIL-101(Cr)-LP (3.5 \text{ mol\% LP}), R.T.}]{\text{HBpin}} R_1R_2CH-NH-R_3 \xrightarrow[\text{neutralization}]{\text{H}_2\text{O or 1 M HCl}} R_1R_2CH_2-NH-R_3$

Entry	Substrate	Code	Yield	Yield ^a
1		2a	38% ^b	87% ^b
2		3a	100% ^b	85% ^b
3		4a	22% ^b	91% ^b
4		5a	42% ^c	60% ^c
5		6a	0% ^c	29% ^c

Reaction conditions: 20 mg MIL101(Cr)-LP (3.5 mol % LP) for heterogeneous or 3.5 mol % LP for homogeneous catalytic reaction, 55 mg (0.43 mmol) HBPin, 0.35 mmol substrate, 3 mL toluene.

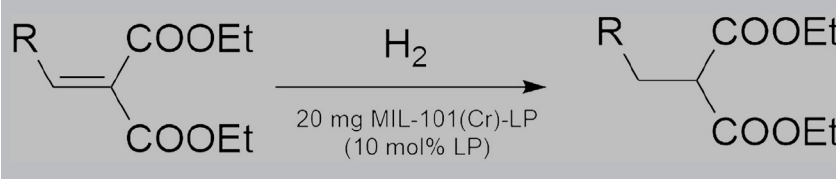
^aYield for the reaction catalyzed by the homogeneous catalyst; this yield is relative to substrate (see [Supplemental Information](#)).

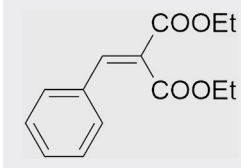
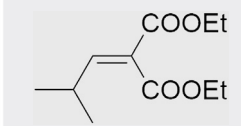
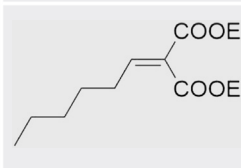
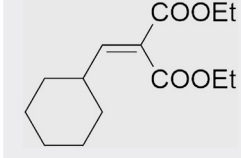
^bReaction time: 3 hr.

^cReaction time: 24 hr.

directly using H₂ gas. Alkylidene malonate compounds with different substituted groups were used to investigate the catalytic performance of the heterogeneous MIL-101(Cr)-LP. As presented in [Table 3](#), the reaction yields catalyzed by MIL-101(Cr)-LP from related alkylidene malonate compounds are 95% for diethyl 2-benzylidenemalonate (**7a**), 84% for diethyl 2-(2-methylpropylidene)malonate (**8a**), 83% for diethyl 2-hexylidenemalonate (**9a**), and 88% for diethyl 2-(cyclohexylmethylene)malonate (**10a**). For comparison, the yields are 92%, 79%, 81%, and 79% when catalyzed by 10 mol % homogeneous FLP catalyst, respectively. The comparison of the yields of these products indicates the MIL-101(Cr)-LP can be used as a porous FLP catalyst and exhibits excellent catalytic performance in the FLP-promoted hydrogenation.

Table 3. Catalysis Studies for Hydrogenation of Alkylidene Malonates



Entry	Substrate	Code	Yield ^a	Yield ^b
1		7a	95%	91%
2		8a	83%	80%
3		9a	81%	79%
4		10a	88%	82%

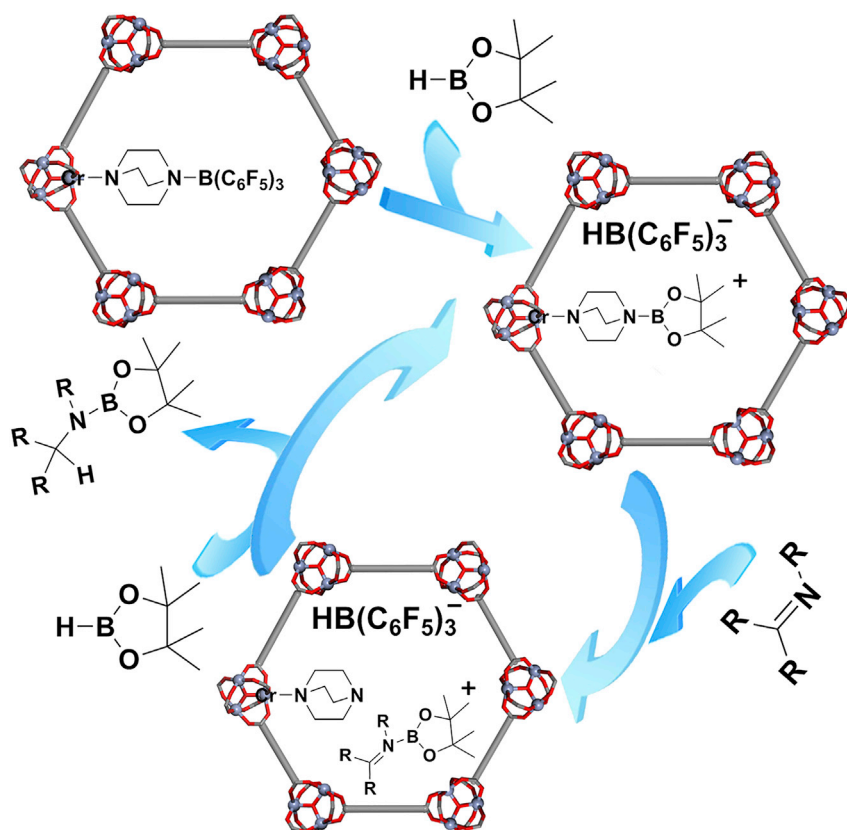
Reaction conditions: 20 mg MIL101(Cr)-LP (10 mol % LP) for heterogeneous or DABCO/B(C₆F₅)₃ (10 mol %) for homogeneous catalytic reaction, 0.12 mmol substrate, 3 mL toluene, 80°C, 24 hr, H₂ 60 bar.

^aYields of isolated product.

^bYield for the reaction catalyzed by the homogeneous catalyst; this yield is relative to the substrate (see Supplemental Information).

Tentative Catalytic Mechanism of MIL-101(Cr)-LP

To investigate the impact of the porous framework structure on the catalysis performance of LP, we examined the kinetics of the reduction of imine **1a** with HBPIn using heterogeneous MIL-101(Cr)-LP and homogeneous LP counterpart. As shown in Figure S13, the reactions catalyzed by both heterogeneous and homogeneous catalysts are on the same order of magnitude; MIL-101(Cr)-LP showed a slower reaction rate as expected due to the additional diffusion process needed for the substrates and products throughout the MOF pores. It is noteworthy that the similar kinetics behaviors of MIL-101(Cr)-LP and the homogeneous LP counterpart implies that MIL-101(Cr)-LP catalyst shares a similar reaction mechanism with that of a homogeneous reaction system.¹⁰ As shown in Scheme 2, the reaction starts with the generation of DABCO-borenium ion, then the borenium ion part transfers from DABCO-borenium ion to imine. The resulting B-activated iminium ion is then reduced by HBPIn with assistance from the Lewis base of MIL-101(Cr)-LP. Reduction of imine-Bpin ion regenerates the borenium ion catalyst, which then reenters the catalytic cycle. The solid-state ¹⁹F NMR of MIL-101(Cr)-LP was used to investigate [HB(C₆F₅)₃]⁻ in the catalytic reactions. After 10 min of starting the reaction, the MIL-101(Cr)-LP was separated and dried for the solid-state ¹⁹F NMR



Scheme 2. Tentative Mechanism for the Reduction Reaction Catalyzed by MIL-101(Cr)-LP

measurement. As shown in Figure S14, the peaks from -125 to 170 ppm match the reported ^{19}F NMR of $[\text{HB}(\text{C}_6\text{F}_5)_3]^-$.¹⁰ The results of solid-state ^{19}F NMR confirmed the intermediate $[\text{HB}(\text{C}_6\text{F}_5)_3]^-$ in the catalytic reactions, thus supporting the above catalyst mechanism.

Recycling Performance of MIL-101(Cr)-LP

Given that the recyclability and long-term stability of the catalyst are the essential performance metrics for cost-effective industrial processes, we investigated these properties for MIL-101(Cr)-LP. Due to the existence of coordination bonds between LP and MOF, the LP leaching is dispelled, given that there are no observable signals of LP in the liquid NMR spectrum of the supernatant after the reaction (Figure S17). Moreover, MIL-101(Cr)-LP can readily be recycled with the steady catalytic performance for at least seven cycles, thus highlighting the heterogeneous nature of the catalytic process (Figure 4). The ^1H NMR data of the decomposed MIL-101(Cr)-LP in 5 wt % NaOH D_2O solution after seven cycles of catalytic reaction matches the original MIL-101(Cr)-LP, thus reinforcing the idea that the LP is competently bound to the Cr sites (Figure S18). The robustness of the catalyst was further confirmed by the well-retained crystallinity and pore structure in MIL-101-LP after the catalytic reaction, as shown by PXRD and N_2 adsorption studies, respectively (Figures S15 and S16).

DISCUSSION

In summary, we have demonstrated the successful grafting of a LP into a MOF via a stepwise anchoring strategy. As a result of the strong coordination interaction between LP and MOF, the LP is stabilized, thereby exhibiting efficient catalytic activity

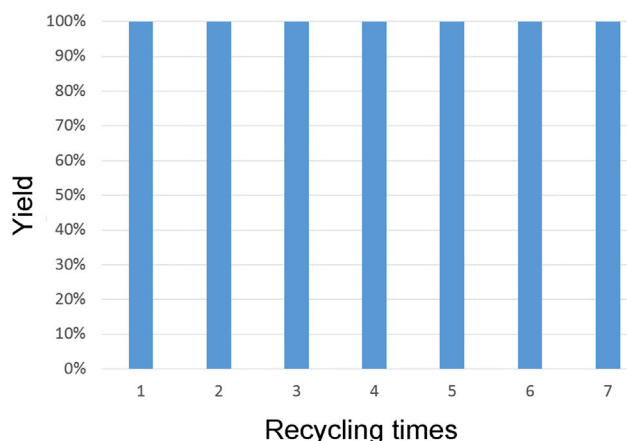


Figure 4. Recycling Performance of MIL-101(Cr)-LP

Reaction conditions: 20 mg MIL-101(Cr)-LP, 55 mg HBPIn, 56 mg **1a**, 3 mL toluene, room temperature, 2 hr.

for catalytic reduction of imines with excellent recyclability. Moreover, interesting size and steric selectivity have also been observed in the catalytic reduction reactions as a result of the confinement imparted by the porous MOF framework structure. Given the broad applicability of LPs, our work therefore lays a foundation for developing MOF-LP as a new paradigm for catalysis. Ongoing work in our laboratory includes grafting different types of LPs into MOFs and exploring the MOF-LP system for various catalysis applications.

EXPERIMENTAL PROCEDURES

Materials

All chemical reagents were obtained from commercial sources and, unless otherwise noted, were used as received without further purification. Organic solvents used in this work were further purified and dried following standard procedures prior to use. All of the experiments for the LP were performed in the glove box.

Synthesis of MIL-101(Cr)-LP

In the glove box, DABCO (2.5 mg, 0.022 mmol) was dissolved in anhydrous toluene with degassed MIL-101(Cr) (20 mg) soaked inside and, after 12 hr, the sample was centrifuged and washed with anhydrous toluene three times. The tris(pentafluorophenyl)borane (15.4 mg, 0.03 mmol) anhydrous toluene solution was added to the sample and then stirred for 12 hr. After that, the sample was centrifuged and washed with anhydrous toluene three times. The sample was then vacuumed for the following catalysis reaction.

Catalytic Reactions

General Procedure for a MIL-101(Cr)-LP-Catalyzed Imine Reduction Reaction (GP1)

In a N₂-filled glove box, MIL-101(Cr)-LP was dispersed into 3 mL of toluene in a 20 mL vial equipped with a small magnetic stir bar. HBPIn was then added to the vial, and substrates were added to the vial after 10 min. The vial was capped and kept in the glove box at room temperature for the noted time. The catalyst was separated by centrifugation. The product was isolated as indicated in the [Supplemental Information](#).

General Procedure for a LP-Catalyzed Imine Reduction Reaction (GP2)

In a N₂-filled glove box, LP was dispersed into 3 mL of toluene in a 20 mL vial equipped with a small magnetic stir bar. HBPIn was then added to the vial, and substrates

were added to the vial after 10 min. The vial was capped and kept in the glove box at room temperature for the noted time. The product was isolated as indicated in the [Supplemental Information](#).

General Procedure for a MIL-101(Cr)-LP-Catalyzed Alkylidene Malonate Hydrogenation Reaction (GP3)

In a N₂-filled glove box, MIL-101(Cr)-LP was dispersed into 2 mL of toluene in a 20 mL vial equipped with a small magnetic stir bar, and then the substrate toluene solution (1 mL) was added to the vial after stirring for 10 min. The resulting mixture was then transferred to the autoclave equipped with the magnetic stir bar. At last, the autoclave was pressurized with H₂ (60 bar) and heated to 80°C for 24 hr. The catalyst was separated by centrifugation. The product was isolated as indicated in the [Supplemental Information](#).

General Procedure for a LP-Catalyzed Alkylidene Malonate Hydrogenation Reaction (GP4)

In a N₂-filled glove box, LP was dispersed into 2 mL of toluene in a 20 mL vial equipped with a small magnetic stir bar, and then the substrates toluene solution (1 mL) was added to the vial after stirring for 10 min. The resulting mixture was then transferred to the autoclave equipped with the magnetic stir bar. The autoclave was then pressurized with H₂ (60 bar) and heated to 80°C for 24 hr. The product was isolated as indicated in the [Supplemental Information](#).

Characterization

Elemental analysis was performed on a PerkinElmer 240 CHN elemental analyzer. Infrared spectra were recorded on a PerkinElmer UATR TWO FTIR spectrophotometer. PXRD measurements were recorded on a Bruker D8 Advance X-ray diffractometer with Cu K α radiation. The simulated powder patterns were calculated with Mercury 2.0. The XPS data were collected on a PHI5000VersaProbe device, the micro scan image and EDS elemental mapping analyses were tested on a ZEISS MERLIN Compact scanning and JEOL JSM-7500F electron microscope. TEM and HAADF-STEM were performed on a Tecnai G² F20 microscope (FEI). The NMR tests were performed on a Varian Unity Inova 400 spectrometer. Gas adsorption measurements were tested by a Micromeritics ASAP 2020 surface area and porosity analyzer.

SUPPLEMENTAL INFORMATION

Supplemental Information includes Supplemental Experimental Procedures, 18 figures, and 1 table and can be found with this article online at <https://doi.org/10.1016/j.chempr.2018.08.018>.

ACKNOWLEDGMENTS

The authors acknowledge the National Science Foundation (DMR-1352065) and the University of South Florida for financial support of this work. Partial support from the National Key R&D Program of China (2016YFB0600902), the National Natural Science Foundation of China (21573267), and the Youth Innovation Promotion Association CAS (2013196) is also acknowledged.

AUTHOR CONTRIBUTIONS

S.M. and Z.N. conceived the research. Z.N. and W.D.C.B.G. synthesized the materials and substrates. Z.N., J.-G.M., Q.S., and Y.C. performed the structural characterizations. Z.N. performed the catalyst reactions and kinetics experiments. The paper

was co-written by S.M., Z.N., P.C.L., B.A., and J.P. All authors discussed the results and commented on the manuscript.

DECLARATION OF INTERESTS

The authors declare no competing interests.

Received: March 26, 2018

Revised: April 24, 2018

Accepted: August 14, 2018

Published: September 27, 2018

REFERENCES AND NOTES

- Stephan, D.W. (2015). Frustrated Lewis pairs. *J. Am. Chem. Soc.* *137*, 10018–10032.
- Stephan, D.W., and Erker, G. (2015). Frustrated Lewis pair chemistry: development and perspectives. *Angew. Chem. Int. Ed.* *54*, 6400–6441.
- Scott, D.J., Fuchter, M.J., and Ashley, A.E. (2017). Designing effective ‘frustrated Lewis pair’ hydrogenation catalysts. *Chem. Soc. Rev.* *46*, 5689–5700.
- Piedra-Arrión, E., Ladaviere, C., Amgoune, A., and Bourissou, D. (2013). Ring-opening polymerization with Zn(C₆F₅)₂-based Lewis pairs: original and efficient approach to cyclic polyesters. *J. Am. Chem. Soc.* *135*, 13306–13309.
- Sun, J., Baylon, R.A., Liu, C., Mei, D., Martin, K.J., Venkatasubramanian, P., and Wang, Y. (2016). Key roles of Lewis acid–base pairs on Zn₂Zr₂O₇ in direct ethanol/acetone to isobutene conversion. *J. Am. Chem. Soc.* *138*, 507–517.
- Axenov, K.V., Kehr, G., Frohlich, R., and Erker, G. (2009). Catalytic hydrogenation of sensitive organometallic compounds by antagonistic N/B Lewis pair catalyst systems. *J. Am. Chem. Soc.* *131*, 3454–3455.
- Knaus, M.G., Giuman, M.M., Pothig, A., and Rieger, B. (2016). End of frustration: catalytic precision polymerization with highly interacting Lewis pairs. *J. Am. Chem. Soc.* *138*, 7776–7781.
- Zhu, J.B., and Chen, E.Y. (2015). From meso-lactide to isotactic polylactide: epimerization by B/N Lewis pairs and kinetic resolution by organic catalysts. *J. Am. Chem. Soc.* *137*, 12506–12509.
- Wisichert, R., Coperet, C., Delbecq, F., and Sautet, P. (2011). Optimal water coverage on alumina: a key to generate Lewis acid–base pairs that are reactive towards the C=H bond activation of methane. *Angew. Chem. Int. Ed.* *50*, 3202–3205.
- Eisenberger, P., Bailey, A.M., and Crudden, C.M. (2012). Taking the F out of FLP: simple Lewis acid–base pairs for mild reductions with neutral boranes via borenium ion catalysis. *J. Am. Chem. Soc.* *134*, 17384–17387.
- Ledoux, A., Larini, P., Boisson, C., Monteil, V., Raynaud, J., and Lacote, E. (2015). Polyboramines for hydrogen release: polymers containing Lewis pairs in their backbone. *Angew. Chem. Int. Ed.* *54*, 15744–15749.
- Trunk, M., Teichert, J.F., and Thomas, A. (2017). Room-temperature activation of hydrogen by semi-immobilized frustrated Lewis pairs in microporous polymer networks. *J. Am. Chem. Soc.* *139*, 3615–3618.
- Xing, J.Y., Buffet, J.C., Rees, N.H., Norby, P., and O’Hare, D. (2016). Hydrogen cleavage by solid-phase frustrated Lewis pairs. *Chem. Commun.* *52*, 10478–10481.
- Li, B., Wen, H.-M., Cui, Y., Zhou, W., Qian, G., and Cheng, B. (2016). Emerging multifunctional metal–organic framework materials. *Adv. Mater.* *28*, 8819–8860.
- Jiang, J., and Yaghi, O.M. (2015). Brønsted acidity in metal–organic frameworks. *Chem. Rev.* *115*, 6966–6997.
- Corma, A., García, H., and Llabrés i Xamena, F.X. (2010). Engineering metal organic frameworks for heterogeneous catalysis. *Chem. Rev.* *110*, 4606–4655.
- Zhou, H.-C., and Kitagawa, S. (2014). Metal–organic frameworks (MOFs). *Chem. Soc. Rev.* *43*, 5415–5418.
- He, H., Perman, J.A., Zhu, G., and Ma, S. (2016). Metal–organic frameworks for CO₂ chemical transformations. *Small* *12*, 6309–6324.
- Liu, J., Chen, L., Cui, H., Zhang, J., Zhang, L., and Su, C.-Y. (2014). Applications of metal–organic frameworks in heterogeneous supramolecular catalysis. *Chem. Soc. Rev.* *43*, 6011–6061.
- Xia, Q., Li, Z., Tan, C., Liu, Y., Gong, W., and Cui, Y. (2017). Multivariate metal–organic frameworks as multifunctional heterogeneous asymmetric catalysts for sequential reactions. *J. Am. Chem. Soc.* *139*, 8259–8266.
- Sheng, J.-Q., Liao, P.-Q., Zhou, D.-D., He, C.-T., Wu, J.-X., Zhang, W.-X., Zhang, J.-P., and Chen, X.-M. (2017). Modular and stepwise synthesis of a hybrid metal–organic framework for efficient electrocatalytic oxygen evolution. *J. Am. Chem. Soc.* *139*, 1778–1781.
- McGuirk, C.M., Katz, M.J., Stern, C.L., Sarjeant, A.A., Hupp, J.T., Farha, O.K., and Mirkin, C.A. (2015). Turning on catalysis: incorporation of a hydrogen-bond-donating squaramide moiety into a Zr metal–organic framework. *J. Am. Chem. Soc.* *137*, 919–925.
- Li, F.-L., Shao, Q., Huang, X., and Lang, J.-P. (2018). Nanoscale trimetallic metal–organic frameworks enable efficient oxygen evolution electrocatalysis. *Angew. Chem. Int. Ed.* *57*, 1888–1892.
- Yu, X., and Cohen, S.M. (2016). Photocatalytic metal–organic frameworks for selective 2,2,2-trifluoroethylation of styrenes. *J. Am. Chem. Soc.* *138*, 12320–12323.
- Thacker, N.C., Lin, Z., Zhang, T., Gilhula, J.C., Abney, C.W., and Lin, W. (2016). Robust and porous β-diketiminato-functionalized metal–organic frameworks for earth-abundant-metal-catalyzed C–H amination and hydrogenation. *J. Am. Chem. Soc.* *138*, 3501–3509.
- Lun, D.J., Waterhouse, G.I., and Telfer, S.G. (2011). A general thermolabile protecting group strategy for organocatalytic metal–organic frameworks. *J. Am. Chem. Soc.* *133*, 5806–5809.
- He, J., Waggoner, N.W., Dunning, S.G., Steiner, A., Lynch, V.M., and Humphrey, S.M. (2016). A PCP pincer ligand for coordination polymers with versatile chemical reactivity: selective activation of CO₂ gas over CO gas in the solid state. *Angew. Chem. Int. Ed.* *55*, 12351–12355.
- Manna, K., Ji, P., Greene, F.X., and Lin, W. (2016). Metal–organic framework nodes support single-site magnesium–alkyl catalysts for hydroboration and hydroamination reactions. *J. Am. Chem. Soc.* *138*, 7488–7491.
- Burgess, S.A., Kassie, A., Baranowski, S.A., Fritzsche, K.J., Schmidt-Rohr, K., Brown, C.M., and Wade, C.R. (2016). Improved catalytic activity and stability of a palladium pincer complex by incorporation into a metal–organic framework. *J. Am. Chem. Soc.* *138*, 1780–1783.
- Wang, L., Agnew, D.W., Yu, X., Figueroa, J.S., and Cohen, S.M. (2018). A metal–organic framework with exceptional activity for C–H bond amination. *Angew. Chem. Int. Ed.* *57*, 511–515.
- Liu, Y., Xi, X., Ye, C., Gong, T., Yang, Z., and Cui, Y. (2014). Chiral metal–organic frameworks bearing free carboxylic acids for organocatalyst encapsulation. *Angew. Chem. Int. Ed.* *53*, 13821–13825.
- Zhang, T., Manna, K., and Lin, W. (2016). Metal–organic frameworks stabilize solution-inaccessible cobalt catalysts for highly efficient

- broad-scope organic transformations. *J. Am. Chem. Soc.* **138**, 3241–3249.
33. Noh, H., Cui, Y., Peters, A.W., Pahls, D.R., Ortuno, M.A., Vermeulen, N.A., Cramer, C.J., Gagliardi, L., Hupp, J.T., and Farha, O.K. (2016). An exceptionally stable metal–organic framework supported molybdenum (VI) oxide catalyst for cyclohexene epoxidation. *J. Am. Chem. Soc.* **138**, 14720–14726.
34. Huang, G., Yang, Q., Xu, W., Yu, S.-H., and Jiang, H.-L. (2016). Polydimethylsiloxane coating for a palladium/MOF composite: highly improved catalytic performance by surface hydrophobization. *Angew. Chem. Int. Ed.* **55**, 7379–7383.
35. Zhao, M., Yuan, K., Wang, Y., Li, G., Guo, J., Gu, L., Hu, W., Zhao, H., and Tang, Z. (2016). Metal-organic frameworks as selectivity regulators for hydrogenation reactions. *Nature* **539**, 76–80.
36. Saha, S., Das, G., Thote, J., and Banerjee, R. (2014). Photocatalytic metal–organic framework from CdS quantum dot incubated luminescent metallohydrogel. *J. Am. Chem. Soc.* **136**, 14845–14851.
37. Chen, Y.Z., Wang, Z.U., Wang, H., Lu, J., Yu, S.H., and Jiang, H.-L. (2017). Singlet oxygen-engaged selective photo-oxidation over Pt nanocrystals/porphyrinic MOF: the roles of photothermal effect and Pt electronic state. *J. Am. Chem. Soc.* **139**, 2035–2044.
38. Li, X., Zhang, B., Tang, L., Goh, T.W., Qi, S., Volkov, A., Pei, Y., Qi, Z., Tsung, C.-K., Levi, S., and Huang, W. (2017). Cooperative multifunctional catalysts for nitron synthesis: platinum nanoclusters in amine-functionalized metal-organic frameworks. *Angew. Chem. Int. Ed.* **56**, 16371–16375.
39. Xiao, J.-D. (2016). Boosting photocatalytic hydrogen production of a metal–organic framework decorated with platinum nanoparticles: the platinum location matters. *Angew. Chem. Int. Ed.* **55**, 9383–9393.
40. Chen, Y., Lykourinou, V., Vetromile, C., Hoang, T., Ming, L.-J., Larsen, R., and Ma, S. (2012). How can proteins enter the interior of a MOF? Investigation of cytochrome c translocation into a MOF consisting of mesoporous cages with microporous windows. *J. Am. Chem. Soc.* **134**, 13188–13191.
41. Li, P., Moon, S.-Y., Guelta, M.A., Harvey, S.P., Hupp, J.T., and Farha, O.K. (2016). Encapsulation of a nerve agent detoxifying enzyme by a mesoporous zirconium metal–organic framework engenders thermal and long-term stability. *J. Am. Chem. Soc.* **138**, 8052–8055.
42. Liao, F.S., Lo, W.S., Hsu, Y.S., Wu, C.C., Wang, S.C., Shieh, F.K., Morabito, J.V., Chou, L.Y., Wu, K.C., and Tsung, C.K. (2017). Shielding against unfolding by embedding enzymes in metal–organic frameworks via a de novo approach. *J. Am. Chem. Soc.* **139**, 6530–6533.
43. Ye, J., and Johnson, J.K. (2015). Design of Lewis pair-functionalized metal organic frameworks for CO₂ hydrogenation. *ACS Catal.* **5**, 2921–2928.
44. Chen, J., Falivene, L., Caporaso, L., Cavallo, L., and Chen, E.Y. (2016). Selective reduction of CO₂ to CH₄ by tandem hydrosilylation with mixed Al/B catalysts. *J. Am. Chem. Soc.* **138**, 5321–5333.
45. Li, S., Li, G., Meng, W., and Du, H. (2016). A frustrated Lewis pair catalyzed asymmetric transfer hydrogenation of imines using ammonia borane. *J. Am. Chem. Soc.* **138**, 12956–12962.
46. Chen, G.Q., Kehr, G., Muck-Lichtenfeld, C., Daniliuc, C.G., and Erker, G. (2016). Phospho-Claisen type reactions at frustrated Lewis pair frameworks. *J. Am. Chem. Soc.* **138**, 8554–8559.
47. Férey, G., Mellot-Draznieks, C., Serre, C., Millange, F., Dutour, J., Surlé, S., and Margiolaki, I. (2005). A chromium terephthalate-based solid with unusually large pore volumes and surface area. *Science* **309**, 2040–2042.
48. Liu, X.H., Ma, J.G., Niu, Z., Yang, G.M., and Cheng, P. (2015). An efficient nanoscale heterogeneous catalyst for the capture and conversion of carbon dioxide at ambient pressure. *Angew. Chem. Int. Ed.* **54**, 988–991.
49. Guo, Q., Ren, L., Kumar, P., Cybulskis, V.J., Mkhoyan, K.A., Davis, M.E., and Tsapatsis, M. (2018). A chromium hydroxide/MIL-101(Cr) MOF composite catalyst and its use for the selective isomerization of glucose to fructose. *Angew. Chem. Int. Ed.* **57**, 4926–4930.
50. Ding, M., and Jiang, H.-L. (2018). Incorporation of imidazolium-based poly(ionic liquids) into a metal-organic framework for CO₂ capture and conversion. *ACS Catal.* **8**, 3194–3201.
51. Inés, B., Palomas, D., Holle, S., Steinberg, S., Nicasio, J.A., and Alcarazo, M. (2012). Metal-free hydrogenation of electron-poor allenes and alkenes. *Angew. Chem. Int. Ed.* **51**, 12367–12369.
52. Bromberg, L., Diao, Y., Wu, H., Speakman, S.A., and Hatton, T.A. (2012). Chromium(III) terephthalate metal organic framework (MIL-101): HF-free synthesis, structure, polyoxometalate composites, and catalytic properties. *Chem. Mater.* **24**, 1664–1675.
53. Luo, Q., Li, M., Lu, M., Hao, C., Qiu, J., and Li, Y. (2013). Organic electron-rich N-heterocyclic compound as a chemical bridge: building a Brønsted acidic ionic liquid confined in MIL-101 nanocages. *J. Mater. Chem. A* **1**, 6530–6534.
54. Hwang, Y.K., Hong, D.Y., Chang, J.S., Jhung, S.H., Seo, Y.K., Kim, J., Vimont, A., Daturi, M., Serre, C., and Férey, G. (2008). Amine grafting on coordinatively unsaturated metal centers of MOFs: consequences for catalysis and metal encapsulation. *Angew. Chem. Int. Ed.* **47**, 4144–4148.
55. De Vries, T.S., Prokofjevs, A., and Vedejs, E. (2012). Cationic tricoordinate boron intermediates: borenium chemistry from the organic perspective. *Chem. Rev.* **112**, 4246–4282.
56. Prokofjevs, A., Boussonniere, A., Li, L., Bonin, H., Lacote, E., Curran, D.P., and Vedejs, E. (2012). Borenium ion catalyzed hydroboration of alkenes with N-heterocyclic carbene-borane. *J. Am. Chem. Soc.* **134**, 12281–12288.
57. Frey, G.D., Lavallo, V., Donnadiou, B., Schoeller, W.W., and Bertrand, G. (2007). Facile splitting of hydrogen and ammonia by nucleophilic activation at a single carbon center. *Science* **16**, 439–441.
58. Reddy, J.S., Xu, B.H., Mahdy, T., Frçhlich, R., Kehr, G., Stephan, D.W., and Erker, G. (2012). Alkenylborane-derived frustrated Lewis pairs: metal-free catalytic hydrogenation reactions of electron-deficient alkenes. *Organometallics* **31**, 5638–5649.